

SUPPORTING INFORMATION FOR

Highly Sensitive Single Domain Antibody-Quantum Dot Conjugates for Detection of HER2 Biomarker in Lung and Breast Cancer Cells

Tatsiana Y. Rakovich,^{†} Omar K. Mahfoud,[†] Bashir M. Mohamed,[†] Adriele Prina-Mello,^{†§}
Kieran Crosbie-Staunton,[†] Tina Van Den Broeck,[¶] Line De Kimpe,[¶] Alyona Sukhanova,^{¶†} Daniel
Baty,[¶] Aliaksandra Rakovich,[‡] Stefan A. Maier,[‡] Frauke Alves,[±] Frans Nauwelaers,[¶] Igor Nabiev,
^{¶†} Patrick Chames,[¶] Yuri Volkov^{†§}*

[†] School of Medicine, Department of Clinical Medicine, Institute of Molecular Medicine, Trinity College, Dublin 8, Ireland, [§]Centre for Research on Adaptive Nanostructures and Nanodevices, Trinity College, Dublin 2, Ireland, [‡]Physics Department, Imperial College, London SW7 2AZ, UK, [¶]BD Biosciences, Erembodegem-Dorp 86, B-9320 Erembodegem, Belgium, [□]Laboratoire de Recherche en Nanosciences, LRN-EA4682, Université de Reims Champagne-Ardenne, 51100 Reims, France, [±]Laboratory of Nano-Bioengineering, National Research Nuclear University MePhl “Moscow Engineering Physics Institute”, 115409 Moscow, Russian Federation, [¶]CRCM, INSERM U1068, 13009 Marseille, France, [±]Max-Planck Institute for Experimental Medicine, Goettingen, Germany

Contents

Cell models	3
Flow cytometry analysis of fluorescence intensity of HER2 biomarker with different conjugates	5
Cytotoxicity Assay with the use of High Content Screening Analysis	6
Cytotoxicity Assay with the use of flow cytometry.....	6
Flow cytometry analysis of HER2 protein expression in lung and breast cancer cells	7
Abbreviations.....	8
References.....	11

Optical characteristics of sdAbs-QD and mAbs-AF conjugates

The emission bands of the HER2 specific mAbs-Alexa Fluor (AF) 488 (dashed line in Figure 4A) and mAbs-AF568 (dashed line in Figure 4B) conjugates were found to be spectrally much broader than those of the HER2 specific sdAbs-QD conjugates (dashed line in Figure 4C). In particular, the emission spectra of mAbs-AF488 and mAbs-AF568 extended over approximately 160 nm range (see broken line in Figure 4A&B, respectively), while in contrast sdAbs-QD conjugates' emission was relatively narrow and confined to 100 nm window (Figure 4C). In multiplexing applications, this narrower and symmetric emission of sdAbs-QD conjugates can allow for better deconvolution of signals, thus improving the resolution with which differently-labelled cellular components can be concurrently imaged.

Cell models

All of the lung cancer cell lines chosen were from human non-small cell lung carcinoma (NSCLC), an epithelial lung cancer that is quite insensitive to chemotherapy when compared to small cell carcinoma and is the most common type of lung cancer, accounting for 80% of all lung cancers. Two of the most common types of NSCLC are squamous cell carcinoma and adenocarcinoma. Squamous cell carcinoma occurs more frequently in men than women and are usually centrally localised within larger bronchi. Incidence of this subset is higher in smokers compared to all other types of lung cancers.¹ Adenocarcinoma is one of the most common types of lung cancer in lifelong non-smokers that is often found in the periphery of lungs and accounts for approximately 40% of lung cancers.² For the purpose of this study each lung cancer cell model used represents different types of NSCLC. A549 cell model is an adenocarcinoma human alveolar basal epithelial cell line that was initiated through explant culture of lung carcinomatous

tissue.³ The NCI-H520 cell line was derived from a sample of a lung mass taken from a patient with squamous cell carcinoma of the lung. The NCI-H596 cell line was derived from a tumour mass in the chest wall of a patient with adenosquamous carcinoma of the lung.⁴

All breast cancer cell models chosen for this study were extracted from mammary gland/breast and were of invasive ductal carcinoma (IDC) origin, a type of breast cancer that accounts for 80% of diagnosed breast cancer cases. IDC initiates in the breast ducts and if left untreated can invade the surrounding breast tissue and metastasise. The BT-474 cell line was isolated from a solid, invasive ductal carcinoma of the breast and SK-BR-3 and MDA-MB-231 were derived from metastatic site where pleural effusion was observed.⁴

Table S1. Lung and breast cancer cell models

Type of Cancer	Positive Cell Lines of Choice	Negative Cell Lines of Choice
Lung	NCI-H596	NCI-H520
	A549	
Breast	SK-BR-3	MDA-MB-231
	BT-474	

Flow cytometry analysis of fluorescence intensity of HER2 biomarker with different conjugates

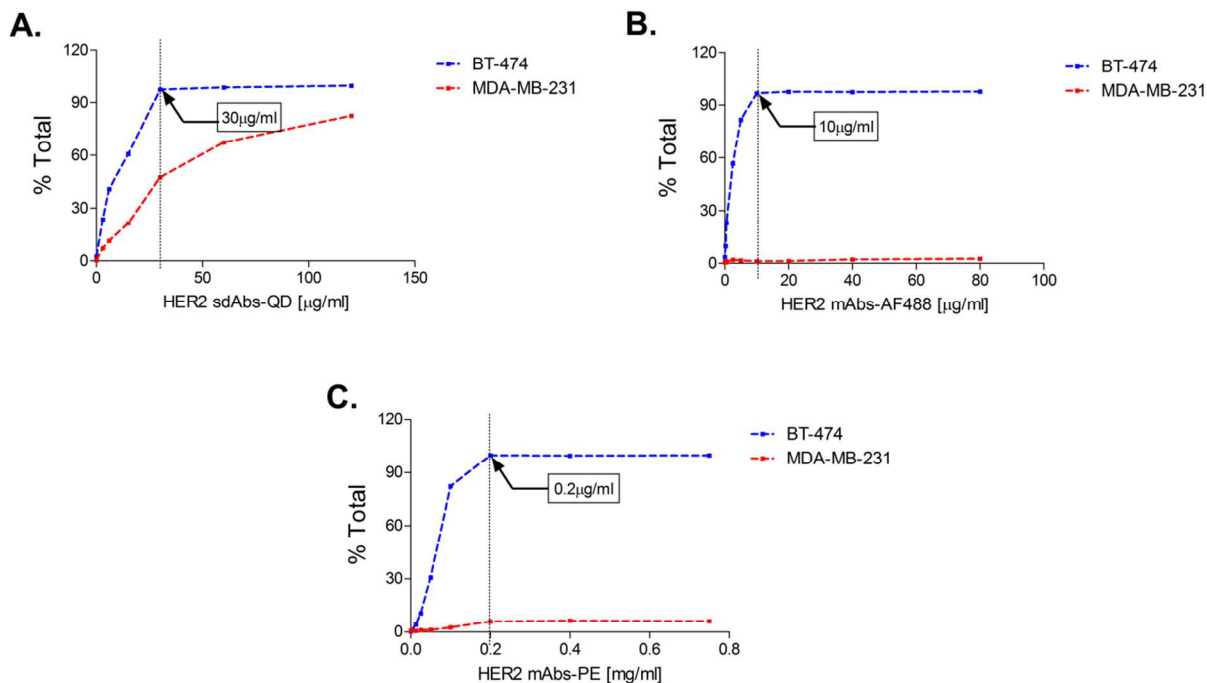


Figure S1. Flow cytometric analysis of fluorescent intensity of HER2 biomarker in breast cancer cell lines (BT-474 and MDA-MB-231) with the use of HER2 specific mAbs-AF488 (A), mAbs-PE (B) conjugates and comparison to sdAbs-QD (C) conjugates.

With all three antibody conjugates tested, high HER2 expressing BT-474 cell line showed a concentration dependent increase in %TSI while MDA-MB-231 cell line showed no change in %TSI (Figure S1A&B).

Similar to the result obtained with mAbs-AF488 and mAbs-PE, staining with sdAbs-QD conjugates resulted in %TSI increase in positive BT-474 breast cancer cell line with increasing QD concentration (Figure S1C). A slight concentration dependent increase in %TSI in MDA-MB-231 cell line was also observed but was found to be much poorer than that of a positive cell line and correlated with the results obtained when carrying out ELISA analysis of whole protein

cell extracts (Figure 2). In literature, MDA-MB-231 breast cell line is also considered to be either negative for HER2 expression,^{5,6} or weakly positive.^{7,8}

Cytotoxicity Assay with the use of High Content Screening Analysis

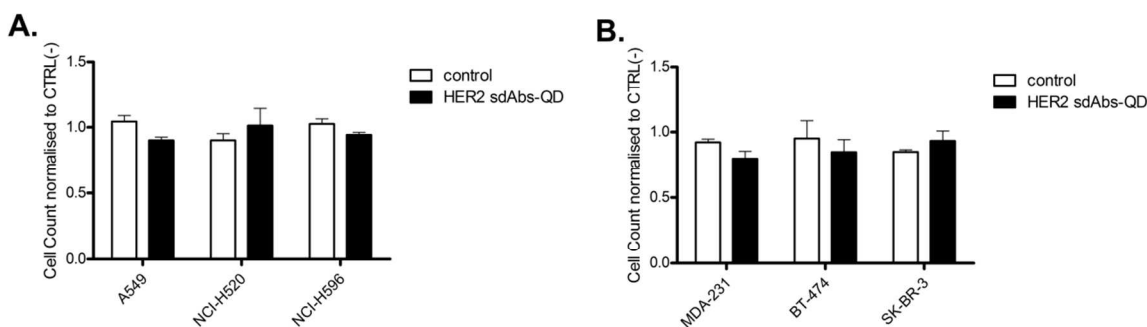


Figure S2. Cytotoxicity Assay of HER2 specific sdAbs-QD and gp120 specific sdAbs-QD in lung and breast cancer cell lines. A) Graph of cell count normalised to negative control CTRL- (untreated cells) in lung cancer cell lines (A549, NCI-H520 and NCI-H596) and B) in breast cancer cell lines (MDA_MB-231, BT-474 and SK-BR-3), determined and analysed with the use of high content screening system.

Cytotoxicity Assay with the use of flow cytometry

Table S2. Percentage of cell death upon incubation of MDA-MB-231 with HER2 specific sdAbs-QD conjugates.

HER2 sdAbs-QD [$\mu\text{g/ml}$]	%Death MDA-MB-231
0	11.5
0.75	11.2
1.50	12.1
3.00	8.8

6.00	11.3
15.00	9.9
30.00	10.7
60.00	12.0
120.00	16.0

HER2 specific sdAbs-QD conjugates were incubated for 1h at 4°C with 100,000 cells at the indicated concentrations (in 50 μ l). During the last 10 minutes, 7-AAD was added and the % of dead cells was quantified.

Flow cytometry analysis of HER2 protein expression in lung and breast cancer cells

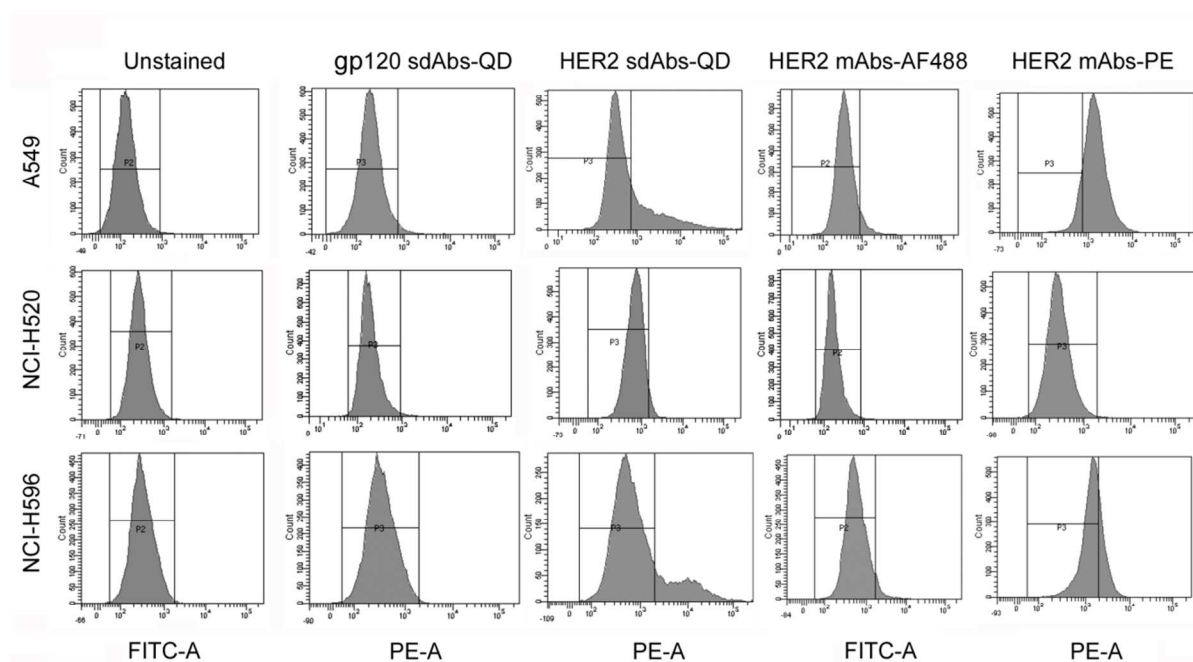


Figure S3. Flow cytometry analysis of HER-2 protein expression in positive (A549 and NCI-H596) and negative (NCI-H520) lung cancer cell models. Cells were labeled with HER2 specific mAbs-AF488, mAbs-PE, sdAbs-QD and gp120 specific sdAbs-QD conjugates. gp120 specific

sdAbs-QD conjugates were used as control for non-specific QD binding (10,000 events per run, n=3).

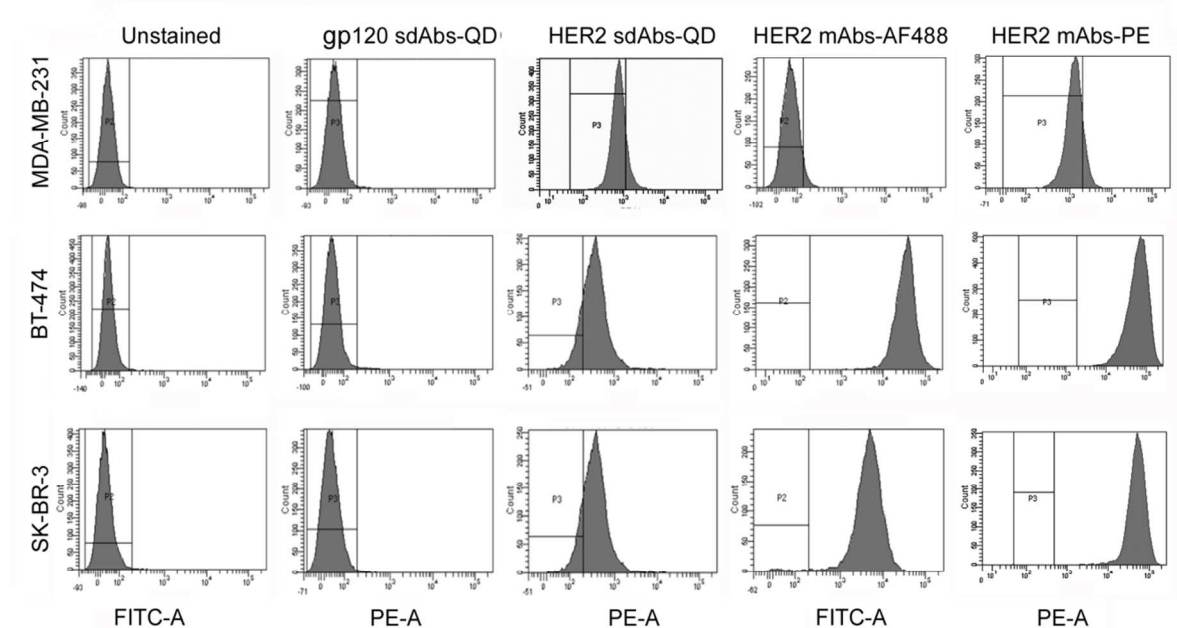


Figure S4. Flow cytometry analysis of HER-2 protein expression in positive (BT-474 and SK-BR-3) and negative (MDA-MB-231) breast cancer cell models. Cells were labeled with HER2 specific mAbs-AF488, mAbs-PE, sdAbs-QD and gp120 specific sdAbs-QD conjugates. gp120 specific sdAbs-QD conjugates were used as control for non-specific QD binding (10,000 events per run, n=3).

Abbreviations

HER2	Human Epidermal Growth Factor Receptor 2
%TSI	Percentage of total staining intensity
µg	microgram

μl	microliter
7-AAD	7-Aminoactinomycin D
Ab	antibody
Abs	antibodies
AF	Alexa Fluor
APC	Allophycocyanin
BD	Becton, Dickinson and Company
Bis-Tris	2-bis(2-hydroxyethyl)amino-2-(hydroxymethyl)-1,3-propanediol
BP	band-pass
BSA	bovine serum albumin
Ca	calcium
CdSe/ZnS	Cadmium Selenide/Zinc Sulphide
CO ₂	Carbon Dioxide
DMEM	Dulbecco's modified Eagle medium
DTT	dithiothreitol
EDTA	Ethylenediaminetetraacetic acid
ELISA	Enzyme-linked immunosorbent assay
FBS	foetal bovine serum
FLIM	Fluorescence-lifetime imaging microscopy
gp120	Envelope glycoprotein gp120
hcAbs	Heavy chain antibodies
HEPES	(4-(2-hydroxyethyl)-1-piperazineethanesulfonic acid)
HIV	Human immunodeficiency virus
HRP	Horseradish peroxidase
IDC	invasive ductal carcinoma
IGEPAL	octylphenoxypolyethoxyethanol
IgG	Immunoglobulin G

LDS sample buffer	lithium dodecyl sulfate sample loading buffer
LP	longpass
mAb	monoclonal antibody
mg	milligram
Mg	Magnesium
min	minutes
ml	milliliter
mM	millimolar
MOPS	3-(N-morpholino)propanesulfonic acid
Na ₃ VO ₄	sodium orthovanadate
NaCl	sodium chloride
NaF	sodium fluoride
NAMDIATREAM	Nanotechnological toolkits for multi-modal disease diagnostics and treatment monitoring
NaN ₃	Sodium azide
nm	nanometer
NP40	Nonidet P-40
ns	nanosecond
NSCLC	non-small cell lung carcinoma
°C	degrees celsius
PBMCs	peripheral blood mononuclear cells
PBS	phosphate buffered saline
PE	Phycoerythrin
PL	photoluminescence
PM	primary macrophages
PMSF	phenylmethanesulfonylfluoride
PVDF	polyvinylidene fluoride
QDs	Quantum Dots

sd	single domain
sdAb	single domain antibody
SDS-PAGE	sodium dodecyl sulfate - polyacrylamide gel electrophoresis
sdAbs-QD	Single domain antibodies conjugated to QD
TBST	Tris buffered saline with Tween 20
Tris-HCl	Tris-hydrochloride
UV	Ultraviolet
V	volts
WB	western blot

References

1. Kenfield, S. A.; Wei, E. K.; Stampfer, M. J.; Rosner, B. A.; Colditz, G. A. Comparison of Aspects of Smoking among the Four Histological Types of Lung Cancer. *Tob. Control* **2008**, *17*, 198–204.
2. Couraud, S.; Zalcman, G.; Milleron, B.; Morin, F.; Souquet, P.-J. Lung Cancer in Never Smokers--a Review. *Eur. J. Cancer* **2012**, *48*, 1299–1311.
3. Giard, D. J.; Aaronson, S. A.; Todaro, G. J.; Arnstein, P.; Kersey, J. H.; Dosik, H.; Parks, W. P. In Vitro Cultivation of Human Tumors: Establishment of Cell Lines Derived From a Series of Solid Tumors. *J Natl Cancer Inst* **1973**, *51*, 1417–1423.
4. ATCC: The Global Bioresource Center http://www.lgcstandards-atcc.org/?geo_country=ie (accessed Apr 4, 2014).
5. Meric, F.; Lee, W.-P.; Sahin, A.; Zhang, H.; Kung, H.-J.; Hung, M.-C. Expression Profile of Tyrosine Kinases in Breast Cancer. *Clin. Cancer Res.* **2002**, *8*, 361–367.

6. Tseng, P.-H.; Wang, Y.-C.; Weng, S.-C.; Weng, J.-R.; Chen, C.-S.; Brueggemeier, R. W.; Shapiro, C. L.; Chen, C.-Y.; Dunn, S. E.; Pollak, M.; *et al.* Overcoming Trastuzumab Resistance in HER2-Overexpressing Breast Cancer Cells by Using a Novel Celecoxib-Derived Phosphoinositide-Dependent Kinase-1 Inhibitor. *Mol. Pharmacol.* **2006**, *70*, 1534–1541.
7. Artemov, D.; Mori, N.; Okollie, B.; Bhujwala, Z. M. MR Molecular Imaging of the Her-2/neu Receptor in Breast Cancer Cells Using Targeted Iron Oxide Nanoparticles. *Magn. Reson. Med.* **2003**, *49*, 403–408.
8. Kunisue, H.; Kurebayashi, J.; Otsuki, T.; Tang, C. K.; Kurosumi, M.; Yamamoto, S.; Tanaka, K.; Doihara, H.; Shimizu, N.; Sonoo, H. Anti-HER2 Antibody Enhances the Growth Inhibitory Effect of Anti-Oestrogen on Breast Cancer Cells Expressing Both Oestrogen Receptors and HER2. *Br. J. Cancer* **2000**, *82*, 46–51.
9. Wang, X.; Ren, X.; Kahen, K.; Hahn, M. A.; Rajeswaran, M.; Maccagnano-Zacher, S.; Silcox, J.; Cragg, G. E.; Efros, A. L.; Krauss, T. D. Non-Blinking Semiconductor Nanocrystals. *Nature* **2009**, *459*, 686–689.